

Energy Difference Controllers for MMC without DC Current Perturbations

Kosei Shinoda, Julian Freytes, Abdelkrim Benchaib, Jing Dai, Hani Saad, Xavier Guillaud

▶ **To cite this version:**

Kosei Shinoda, Julian Freytes, Abdelkrim Benchaib, Jing Dai, Hani Saad, et al.. Energy Difference Controllers for MMC without DC Current Perturbations. The 2nd International Conference on HVDC (HVDC2016), Sep 2016, Shanghai, China. hal-01423721

HAL Id: hal-01423721

https://centralesupelec.hal.science/hal-01423721

Submitted on 31 Dec 2016

HAL is a multi-disciplinary open access archive for the deposit and dissemination of scientific research documents, whether they are published or not. The documents may come from teaching and research institutions in France or abroad, or from public or private research centers.

L'archive ouverte pluridisciplinaire **HAL**, est destinée au dépôt et à la diffusion de documents scientifiques de niveau recherche, publiés ou non, émanant des établissements d'enseignement et de recherche français ou étrangers, des laboratoires publics ou privés.

Energy Difference Controllers for MMC without DC Current Perturbations

Kosei Shinoda*, Julian Freytes†, Abdelkrim Benchaib*, Jing Dai*‡, Hani Saad§, Xavier Guillaud†
* SuperGrid Institute SAS, 130 rue Léon Blum, 69611 Villeurbanne, France
† Université Lille, Centrale Lille, Arts et Metiers, HEI EA 2697 - L2EP France
‡ Group of Electrical Engineering - Paris (GeePs), UMR CNRS 8507,
CentraleSupélec, Univ. Paris-Sud, Université Paris-Saclay, Sorbonne Universités, UPMC Univ Paris 06, France
§ Réseau de Transport d'Électricité (RTE), La Défense, France

***Abstract*—The Modular Multilevel Converter (MMC) is a most promising converter technology for the High Voltage DC application. The complex topology of the MMC requires several additional controllers to balance the energy in the capacitors which are distributed all over the converter. Typically, there is a requirement of two controls; one is the regulation of the total energy in each leg, and the other is the distribution of the energy between the upper and the lower arms. This paper presents control strategies for the latter one being capable of distributing the energy only by internal power flow, so that undesired interference with the associated grids can be completely avoided. The proposed controls are achieved by forcing the common mode currents to be balanced while keeping the classic cascaded control structure as much as possible. The effectiveness and advantage of the proposed solutions are demonstrated by simulations.**

***Index Terms*—High Voltage Direct Current (HVDC), Modular Multilevel Converter (MMC), Energy Difference.**

I. Introduction

The Modular Multilevel Converter (MMC) is a new type of converter which attracts large attention due to its several advantages compared to the conventional two-level Voltage Source Converter (VSC). MMC was first introduced in [1] and the basic concepts and the operational principles are presented in [2] [3].

The general topology of the MMC consists of a large number of two-level converter modules, so-called sub-modules. This modular topology enables to output nearly ideal sinusoidal voltage waveform, allowing prevention of harmonic injection to the power system; hence, implementation of large filters are no longer needed. Furthermore, its scalable modular topology allows to easily adjust the voltage rating, thus, it is suitable for High Voltage Direct Current (HVDC) Transmission Systems applications.

In general, the conventional VSCs type converters are attached with a large station capacitor at their DC side. In the MMC, however, the capacitors are distributed all over the converter. This makes the balancing and control of the distributed energies as an important aspect [4]. In literature, the requirements on the energy balancing are often divided into two [5] [6]:

1) Horizontal Balancing: The energy stored in each leg must be regulated to achieve equal energy in all three phase legs. This can be achieved by a simple control which regulates the deference between the power inflow and outflows to/from the MMC in each phase.
2) Vertical Balancing: The difference between the energy stored in the upper and the lower parts must be controlled to avoid having an excess energy in one of the arms. This is also refereed to as "Energy Difference Control" [7].

This paper discuss on the control strategies of Energy Difference. The control schemes proposed in [2] and [8] use additional oscillatory components on the common mode currents to regulate this energy difference. However, this approach can result in unwanted interferences with the DC power which may lead to fluctuations of the DC grid voltage. [5] presented a novel control structure utilizing a periodic linear quadratic regulator, and referred to balanced reference generation. Inspired by [5], this paper proposes different control structures, which enables to regulate energy difference without disturbing the DC grid. In this work, the cascaded control structure such that energy controllers adjusting the references of inner current control is preserved. Thus, the proposed controllers are simpler and more intuitive.

This paper is structured as follows. Section 2 recalls the MMC topology and the fundamental variables as well as its control hierarchy. In Section 3, the proposed energy difference controllers are presented, and difference in structure is highlighted. The functionality of the proposed controllers is validated by simulations carried out on EMTP-RV platform.

II. Modular Multilevel Converter

A. Arm Average Model (AAM)

The topology of the AAM is recalled in Fig. 1. There is one leg for each phase a, b, c. Each phase leg can be divided into upper and lower parts called arms. This model assumes that the voltages of all the sub-module capacitors in each arm are maintained in a close range, thus allowing to replace them by an equivalent capacitor. Therefore, each arm includes an arm inductance L_{arm}, an arm resistance R_{arm} and an equivalent capacitor C_{tot} in parallel with a chopper.

The voltages v_{u_j} (v_{l_j}) and currents i_{u_j} (i_{l_j}) of each arm j ($j = a, b, c$) are described by the following equations:

$$v_{u_j} = m_{u_j} v_{Ctotu_j}, \quad v_{l_j} = m_{l_j} v_{Ctotl_j} \tag{1}$$

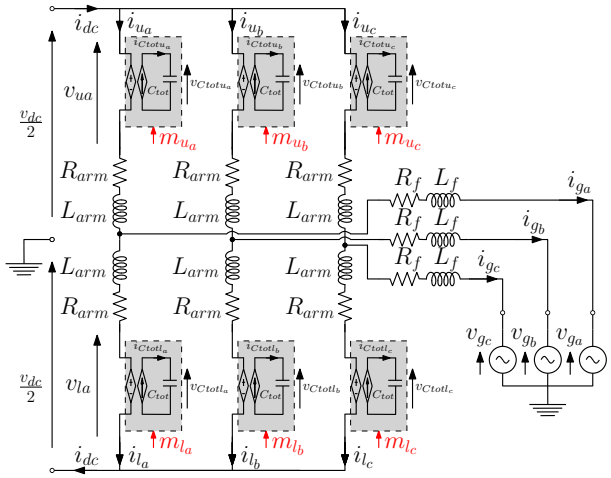


Figure 1: MMC Arm average model

$$i_{Ctotu_j} = m_{u_j} i_{u_j}, \quad i_{Ctotl_j} = m_{l_j} i_{l_j} \tag{2}$$

where v_{Ctotu_j} (v_{Ctotl_j}) is the voltage across the upper (lower) arm equivalent capacitor, m_{u_j} (m_{l_j}) is the corresponding instantaneous duty cycle and i_{Ctotu_j} (i_{Ctotl_j}) is the current through the upper (lower) arm capacitor. The voltage and current of the equivalent capacitor are related through the capacitor equation:

$$i_{Ctotu_j} = C_{tot}\frac{dv_{Ctotu_j}}{dt}, \quad i_{Ctotl_j} = C_{tot}\frac{dv_{Ctotl_j}}{dt} \tag{3}$$

Applying Kirchhoff's law, the following equations are derived for each phase j:

$$\tfrac{v_{dc}}{2} - v_{u_j} - L_{arm}\tfrac{di_{u_j}}{dt} - R_{arm}i_{u_j} - L_f\tfrac{di_{g_j}}{dt} - R_f i_{g_j} - v_{g_j} = 0 \tag{4}$$

$$-\tfrac{v_{dc}}{2} + v_{l_j} + L_{arm}\tfrac{di_{l_j}}{dt} + R_{arm}i_{l_j} - L_f\tfrac{di_{g_j}}{dt} - R_f i_{g_j} - v_{g_j} = 0 \tag{5}$$

The addition of (4) and (5) yields:

$$v_{v_j} - v_{g_j} = L_{eq}^{ac}\frac{di_{g_j}}{dt} + R_{eq}^{ac} i_{g_j} \tag{6}$$

where:

$$i_{g_j} = i_{u_j} - i_{l_j}, \quad v_{v_j} = \frac{-v_{u_j} + v_{l_j}}{2}, \tag{7}$$

$$R_{eq}^{ac} = \frac{R_{arm} + 2R_f}{2}, \quad L_{eq}^{ac} = \frac{L_{arm} + 2L_f}{2} \tag{8}$$

Equation (6) describes the AC side dynamics of the AAM. The subtraction of (4) and (5) gives:

$$\frac{v_{dc}}{2} - \frac{v_{diff_j}}{2} = L_{arm}\frac{di_{diff_j}}{dt} + R_{arm} i_{diff_j} \tag{9}$$

where the differential current i_{diff} and voltage v_{diff} are defined as:

$$i_{diff_j} = \frac{i_{u_j} + i_{l_j}}{2}, \quad v_{diff_j} = \frac{v_{u_j} + v_{l_j}}{2} \tag{10}$$

Equation (9) describes the DC side dynamics of the AAM. The DC current will be then expressed as:

$$i_{dc} = i_{diff_a} + i_{diff_b} + i_{diff_c} \tag{11}$$

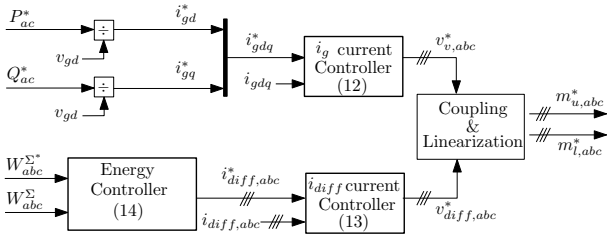


Figure 2: General Control Scheme of MMC

B. Current control and Energy control

For the 3-phase MMC, as well as a classical VSC, the control of i_g is achieved in rotating frame by applying Park transformation. Phase Lock Loop (PLL) is implemented to track the grid voltage angle. The implemented PI controller is denoted as C_{i_g}. Applying Park transformation on (6), the i_g control in dq frame is derived

$$v_{v_d}^* = v_{g_d} + (i_{g_d}^* - i_{g_d})C_{i_g} - \left(\frac{L_{arm}}{2} + L_f\right)\omega i_{g_q} \tag{12a}$$

$$v_{v_q}^* = v_{g_q} + (i_{g_q}^* - i_{g_q})C_{i_g} + \left(\frac{L_{arm}}{2} + L_f\right)\omega i_{g_d}. \tag{12b}$$

The differential current in each phase is regulated by another PI controller C_{idiff}. From (9), the i_{diff} control for phase j is derived as:

$$v_{diff_j}^* = \frac{V_{dc}}{2} - (i_{diff_j}^* - i_{diff_j})C_{i_{diff}}. \tag{13}$$

The difference between the DC power inflow and the AC outflow causes variation of the energy stored inside the MMC. Since it is preferred that the AC power follows the reference value, it is reasonable to adjust the DC power to obtain the desired internal energy level. A PI controller C_{W^Σ} is implemented to give appropriate $i_{diff_j}^*$ to the differential current controllers. The control of W^Σ is obtained as:

$$i_{diff_j}^* = \frac{1}{V_{dc}}\left[\left\{W_j^{\Sigma *} - W_j^{\Sigma}\right\} C_{W^\Sigma} + \frac{P_{ac}}{3}\right] \tag{14}$$

where

$$W_i^{\Sigma} = \frac{1}{2}C_{tot}\left(v_{Ctotu_i}^2 + v_{Ctotl_i}^2\right). \tag{15}$$

Assembling the derived control laws, general control structure is built as shown in Fig. 2.

The developed controller is implemented in a simulation of an MMC station model. The pre-contingency operating power is set at $P_{ac} = 1[p.u.]$ and $Q_{ac} = 0[p.u.]$. Then step reference changes are created at $t = 1[s]$ for the active power and $1.1[s]$ for the reactive power. Fig. 3 shows the transition of the active and reactive powers. It is clearly seen that the both powers follow the change of the reference correctly. Fig. 4 pictures the capacitor voltage in each arm. Even though the capacitor voltages were perfectly balanced beforehand, each time the disturbance occurs, the voltages in the upper arms deviate from the lower ones. This is because the aforementioned energy controller can only regulate the sum of the upper and lower arms' energy, but it does not take into account the distribution

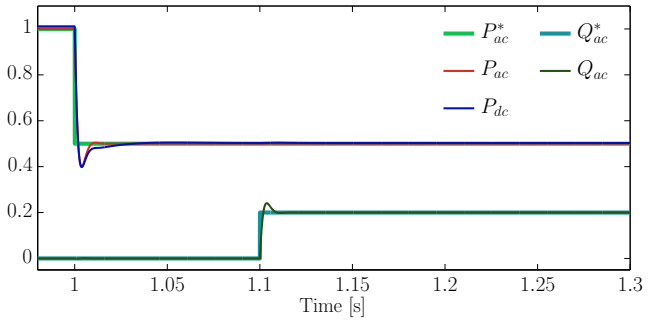


Figure 3: Active power and DC power [pu] - No Energy Difference control

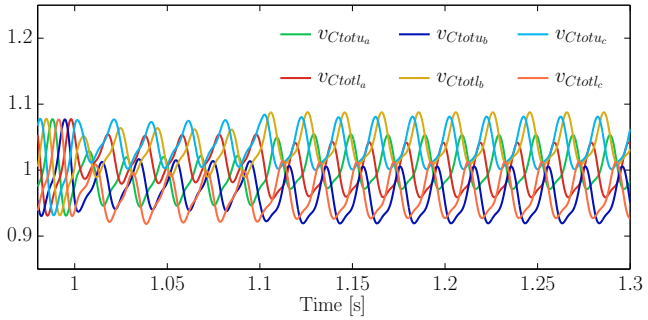


Figure 4: Equivalent arm capacitor voltages [pu]

of the energy between the upper and lower arms. Without explicit control, the energy in the upper and lower arms may take various levels and endanger the secure operation of the MMC. Therefore, an additional controller which enables to explicitly eliminate the deviation of the energy between the arms is needed.

III. Energy difference control

Theoretically, the power exchanged by the arm can be expressed by the product of the applied voltage v_{ul_j} and the current flows through the arms i_{ul_j}. Defining the energy difference by

$$W_j^{\Delta} = \frac{1}{2} C_{tot} \left(v_{Ctotu_j}^2 - v_{Ctotl_j}^2 \right), \tag{16}$$

The evolution of the energy difference can be expressed by using the variables defined in the previous section:

$$\frac{dW_j^{\Delta}}{dt} = i_{u_j} v_{u_j} - i_{l_j} v_{l_j} = i_{g_j} v_{diff_j} - 2 i_{diff_j} v_{v_j}. \tag{17}$$

In normal operation, i_{g_j} and v_{v_j} are sinusoidal with an average of zero, while i_{diff_j} and v_{diff_j} are constant. In such condition, both terms in the right side of (17) are products of a constant value and a fundamental-frequency component. Thus, the time average over the period is zero. This means that, as it is, the energy difference is uncontrollable. One possible solution is to impose fundamental-frequency components on the differential current $(i_{diff} = i_{diff_{ac}} + i_{diff_{dc}})$ [2]. This decomposition allows to generate a non-zero component over the period on the right side of (17), which can be used to regulate the energy difference. Further simplification is done by supposing that v_{v_j} is fairly close to the AC grid voltage v_{g_i} since an MMC does not require large filters at its AC side. Introducing the decomposition of differential current into (17), then the time average of the evolution of the energy difference over one period is expressed by:

$$\left\langle \frac{dW_j^{\Delta}}{dt} \right\rangle = \left\langle -2 i_{diff_{ac_j}} v_{g_j} \right\rangle. \tag{18}$$

From (18), three control laws will be considered. One is the classical control scheme [8]. The second one is developed based on the classical scheme, but the reference generation methods are improved to overcome the problem of the classical scheme. The proposed control is further improved by applying the phase shifting technique proposed by [5]. Each scheme is detailed in the followings.

A. Classical W^{Δ} control

The value of the energy difference can vary for each phase. Therefore, it is reasonable to regulated them individually by implementing one controller for each phase leg. Then the appropriate rms value of the AC components of the differential current $I^*_{diff_{ac}}$ can be derived by a *PI* controller denoted by $C_{W^{\Delta}}$. The control law can be expressed as:

$$I^*_{diff_{ac_j}} = -\frac{1}{2V_g} \left(W_j^{\Delta *} - W_j^{\Delta} \right) C_{W^{\Delta}}. \tag{19}$$

where V_g is the rms value of the AC grid voltage. Next, the fundamental-frequency differential current reference must be generated in some way. The AC voltage angle (i.e. $\theta = \omega t$) is monitored by the PLL and used to align the current reference with the voltage in each arm. In the classical energy difference control, the instantaneous differential current reference $\boldsymbol{i}^*_{diff_{ac}} = \left(i^*_{diff_{ac_a}} i^*_{diff_{ac_b}} i^*_{diff_{ac_c}} \right)^T$ is generated by

$$\boldsymbol{i}^*_{diff_{ac}} = A \boldsymbol{I}^*_{diff_{ac}} \tag{20}$$

where

$$A = \sqrt{2} \begin{bmatrix} \cos \omega t & 0 & 0 \\ 0 & \cos\left(\omega t - \frac{2\pi}{3}\right) & 0 \\ 0 & 0 & \cos\left(\omega t - \frac{2\pi}{3}\right) \end{bmatrix} \tag{21}$$

and $\boldsymbol{I}^*_{diff_{ac}} = \left(I^*_{diff_{ac_a}} I^*_{diff_{ac_b}} I^*_{diff_{ac_c}} \right)^T$. The multiplication with the matrix A allows aligning the output of the controller with the AC grid voltage. Fig. 5 illustrates an example of the relation between the generated current references and the AC grid voltages.

According to (19) and (20), the classic energy difference controller is developed as depicted in Fig. 6. The developed controller is tested in the same simulation set up as previous section. The equivalent arm capacitor voltages are depicted in Fig. 7. Unlike the previous case, the capacitor voltage is well balanced after a short time. However, unwanted oscillations on the DC power are observed in Fig. 8. In this control structure, the energy difference is individually regulated per leg. Since there is no coupling between the phases, the balance

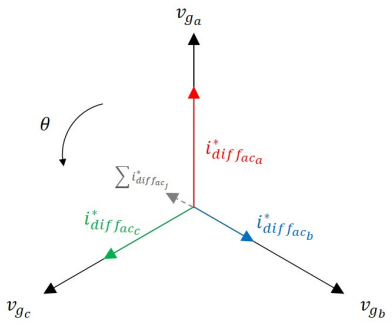


Figure 5: Vectorial representation of differential currents in Classical Control

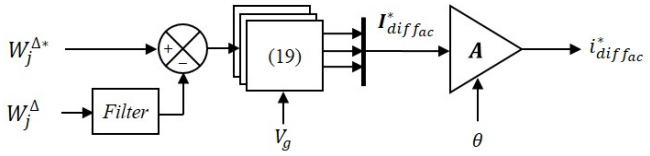


Figure 6: Classical W^{Δ} controller

of them are not guaranteed. As a consequence, unbalanced reference $\boldsymbol{i}^*_{diff_{ac}}$ may possibly be generated by the controller, and it results in inducing oscillations on the DC power. Such oscillations may cause fluctuations on the DC voltage and jeopardize the stability of the entire system, especially in small MTDC grids. Therefore, this must be avoided.

B. W^{Δ} Control with Balanced $\boldsymbol{i}_{diff_{ac}}$

The classical W^{Δ} controller presented in Section III-A may generate unbalanced three-phase current references since the W^{Δ} of each phase is regulated individually. In other words, the current sum $i^{*'}_{diff_{ac_a}} + i^{*'}_{diff_{ac_b}} + i^{*'}_{diff_{ac_c}}$ may be non-zero, which would change the current exchanged with the DC grid. Thus, a new transform is needed so that the new current reference vector, denoted by $\boldsymbol{i}^{*'}_{diff_{ac}}$, with $\boldsymbol{i}^{*'}_{diff_{ac}} = \left(i^{*'}_{diff_{ac_a}} i^{*'}_{diff_{ac_b}} i^{*'}_{diff_{ac_c}}\right)^T$ will have no impact on the external current, i.e. $i^{*'}_{diff_{ac_a}} + i^{*'}_{diff_{ac_b}} + i^{*'}_{diff_{ac_c}} = 0$.

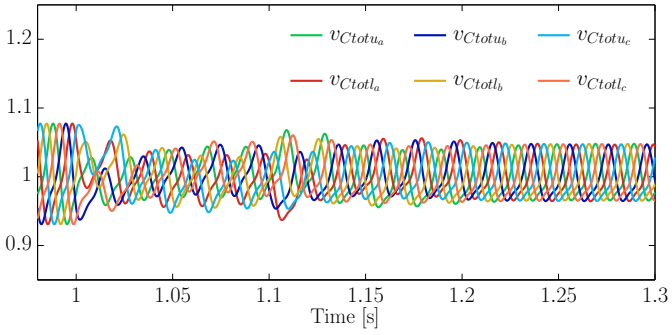


Figure 7: Equivalent arm capacitor voltages [pu] - Classical W^{Δ} control

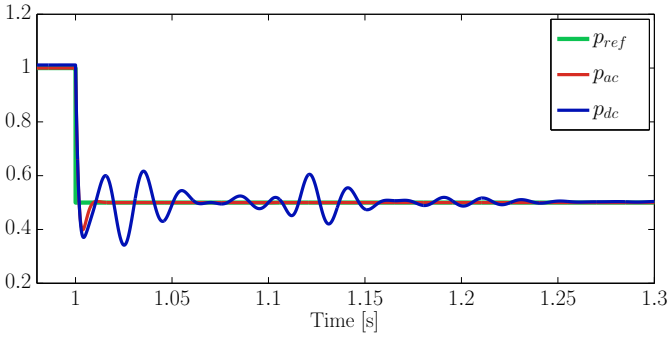


Figure 8: Active power and DC power [pu] - Classical W^{Δ} control

The general principle is that to balance the current reference, for each component of $\boldsymbol{i}^*_{diff_{ac}}$, two new current references are introduced, one for each of the other two phases. Formally, let

$$\boldsymbol{i}^{*'}_{diff_{ac}} = K\boldsymbol{i}^*_{diff_{ac}} = \begin{bmatrix} k_{aa} & k_{ab} & k_{ac} \\ k_{ba} & k_{bb} & k_{bc} \\ k_{ca} & k_{cb} & k_{cc} \end{bmatrix} \boldsymbol{i}^*_{diff_{ac}} \tag{22}$$

where coefficient k_{mn} quantifies the contribution of the original reference $i^*_{diff_{ac_n}}$ to the new reference $i^{*'}_{diff_{ac_m}}$.

This transform should satisfy the following 3 requirements, where we only consider phase a for simplicity:

1) It should not modify the contribution of the original reference to the corresponding phase in the new reference. This yields:
$$k_{aa} = 1$$
2) The new reference should be balanced. This yields:
$$k_{aa} + k_{ba} + k_{ca} = 0$$
3) The absolute values of the two new references in phases b and c should be identical. This yields
$$|k_{ba}| = |k_{ca}|$$

The above 3 requirements allow one to obtain:

$$K = \begin{bmatrix} 1 & -\frac{1}{2} & -\frac{1}{2} \\ -\frac{1}{2} & 1 & -\frac{1}{2} \\ -\frac{1}{2} & -\frac{1}{2} & 1 \end{bmatrix} \tag{23}$$

where we used the symmetry between the three phases.

Fig. 9 shows the compensation of the original current reference $i^*_{diff_{ac_a}}$ for phase a. The colored vectors are defined as $i^{*'}_{diff_{ac_{aa}}} = k_{aa} i^*_{diff_{ac_a}}$, $i^{*'}_{diff_{ac_{ba}}} = k_{ba} i^*_{diff_{ac_a}}$, and $i^{*'}_{diff_{ac_{ca}}} = k_{ca} i^*_{diff_{ac_a}}$. With matrix K given in (23), we see that $i^*_{diff_{ac_a}}$ is well balanced by $i^{*'}_{diff_{ac_{ba}}}$ and $i^{*'}_{diff_{ac_{ca}}}$. The control structure is shown in Fig. 10.

C. Modified W^{Δ} Control with Balanced $\boldsymbol{i}_{diff_{ac}}$

In the W^{Δ} Control with Balanced $\boldsymbol{i}_{diff_{ac}}$, the balancing of the current reference in each phase is achieved by introducing a new current into each of the other two phases. Recall that in Fig. 9, to balance $i^*_{diff_{ac_a}}$ in phase a, $i^{*'}_{diff_{ac_{ba}}}$ and

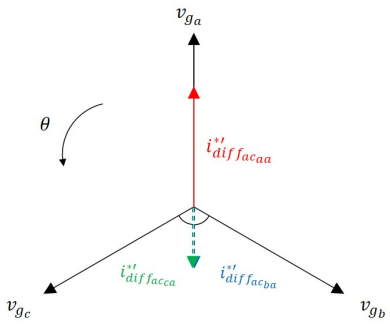


Figure 9: Vectorial representation of differential currents in W^{Δ} Control with Balanced $i_{diff_{ac}}$

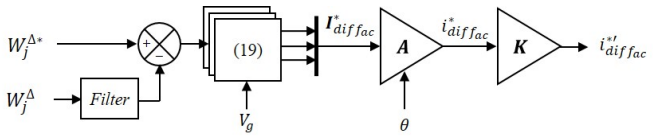


Figure 10: W^{Δ} Controller with Balanced $i_{diff_{ac}}$

$i^{*'}_{diff_{ac_{ca}}}$ are introduced respectively in phases b and c, each with an amplitude of $\frac{1}{2}i^*_{diff_{ac_a}}$. With this choice, $i^{*'}_{diff_{ac_{ba}}}$ and $i^{*'}_{diff_{ac_{ca}}}$ are both phase shifted by 180 degrees with $i^*_{diff_{ac_a}}$ (and thus v_{g_a}), which makes it possible to use a constant matrix K to calculate the new reference vector $\boldsymbol{i}^{*'}_{diff_{ac}}$ from the original one $\boldsymbol{i}^*_{diff_{ac}}$.

Obviously, the choice of $i^{*'}_{diff_{ac_{ba}}}$ and $i^{*'}_{diff_{ac_{ca}}}$ is not unique. As long as their sum is equal to $-i^*_{diff_{ac_a}}$, the new current reference vector is already balanced, although the contributions by phase b and c are no longer bound to be equal. Furthermore, if the constraint on the phase shift of $i^{*'}_{diff_{ac_{ba}}}$ and $i^{*'}_{diff_{ac_{ca}}}$ with respect to $i^*_{diff_{ac_a}}$ is relaxed, i.e. $i^{*'}_{diff_{ac_{ba}}}$ and $i^{*'}_{diff_{ac_{ca}}}$ are allowed to have other directions than $i^*_{diff_{ac_a}}$, then more freedom is permitted in their choice, as long as their vector sum equal to $-i^*_{diff_{ac_a}}$ to guarantee current balance in the three phases. However, in that case, it is no longer possible to use a constant matrix to calculate $\boldsymbol{i}^{*'}_{diff_{ac}}$ from $\boldsymbol{i}^*_{diff_{ac}}$ as in (22). Instead, a time-varying matrix, denoted by M, is needed to calculate $\boldsymbol{i}^{*'}_{diff_{ac}}$ from $\boldsymbol{I}^*_{diff_{ac}}$, i.e.

$$\boldsymbol{i}^{*'}_{diff_{ac}} = M\boldsymbol{I}^*_{diff_{ac}} \tag{24}$$

An example of choosing M is given in [5]. Its objective is to remove power exchanges imposed by the newly introduced current used for balancing, and its general principle is to shift the current vectors by 90 degrees from the corresponding voltage angle. Taking phase a as example, let

$$i^{*'}_{diff_{ac_{aa}}}(t) = l_{aa}\sqrt{2}I^*_{diff_{ac_a}}\cos(\omega t + \phi_a) \tag{25}$$

$$i^{*'}_{diff_{ac_{ba}}}(t) = l_{ba}\sqrt{2}I^*_{diff_{ac_a}}\cos\left(\omega t + \phi_b - \tfrac{2\pi}{3}\right) \tag{26}$$

$$i^{*'}_{diff_{ac_{ca}}}(t) = l_{ca}\sqrt{2}I^*_{diff_{ac_a}}\cos\left(\omega t + \phi_c + \tfrac{2\pi}{3}\right) \tag{27}$$

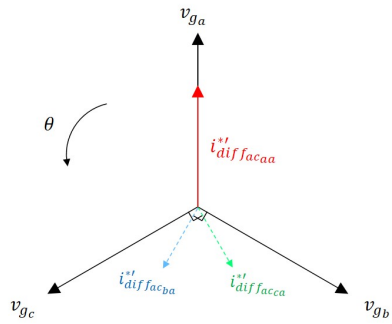


Figure 11: Vectorial representation of differential currents in Modified W^{Δ} Control with Balanced $i_{diff_{ac}}$

where ϕ_m is the phase shift between $i^{*'}_{diff_{ac_{ma}}}$ and the voltage in phase m, and l_{aa}, l_{ba} and l_{ca} are positive[1] constant coefficients.

To determine the value of l_{ma} and ϕ_m, the following requirements are used.

1) The contribution of the original reference to the corresponding phase in the new reference should not be modified. This yields:
$$l_{aa} = 1, \quad \phi_a = 0.$$
2) The new reference should be balanced. This yields:
$$l_{aa}\cos(\omega t + \phi_a) + l_{ba}\cos\left(\omega t + \phi_b - \tfrac{2\pi}{3}\right) + l_{ca}\cos\left(\omega t + \phi_c + \tfrac{2\pi}{3}\right) = 0$$
3) The instantaneous active powers due to $i^{*'}_{diff_{ac_{ba}}}$ and $i^{*'}_{diff_{ac_{ca}}}$ in phases b and c are zero. This yields:
$$l_{ba}V_g I^*_{diff_{ac_a}}\cos\phi_b = l_{ca}V_g I^*_{diff_{ac_a}}\cos\phi_c = 0$$
4) The absolute values of the two new references in phases b and c should be identical. This yields
$$l_{ba} = l_{ca}$$

The above four requirements allow one to obtain

$$l_{aa} = 1, \quad l_{ba} = l_{ca} = \frac{1}{\sqrt{3}}, \quad \phi_a = 0 \quad \phi_b = -\frac{\pi}{2}, \quad \phi_c = \frac{\pi}{2}. \tag{28}$$

By symmetry between the three phases, M can be obtained as

$$M = \sqrt{2}\begin{bmatrix} \cos\omega t & \frac{1}{\sqrt{3}}\cos\left(\omega t + \frac{\pi}{2}\right) & \frac{1}{\sqrt{3}}\cos\left(\omega t - \frac{\pi}{2}\right) \\ \frac{1}{\sqrt{3}}\cos\left(\omega t - \frac{7\pi}{6}\right) & \cos\left(\omega t - \frac{2\pi}{3}\right) & \frac{1}{\sqrt{3}}\cos\left(\omega t - \frac{\pi}{6}\right) \\ \frac{1}{\sqrt{3}}\cos\left(\omega t + \frac{7\pi}{6}\right) & \frac{1}{\sqrt{3}}\cos\left(\omega t + \frac{\pi}{6}\right) & \cos\left(\omega t + \frac{2\pi}{3}\right) \end{bmatrix} \tag{29}$$

Fig. 11 illustrates the generated current reference by the coupling matrix M with phase a as example. The vectors $i^{*'}_{diff_{ac_{ba}}}$ and $i^{*'}_{diff_{ac_{ca}}}$ satisfy the above four requirements.

According to (24) with M given in (29), the control structure is developed as illustrated in Fig. 12.

[1]This can always be achieved by properly choosing ϕ_m.

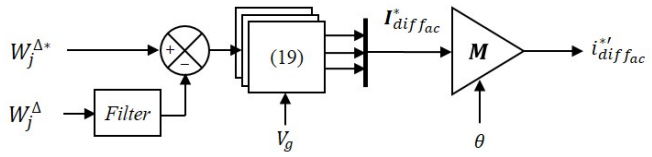


Figure 12: Modified W^{Δ} Controller with Balanced $i_{diff_{ac}}$

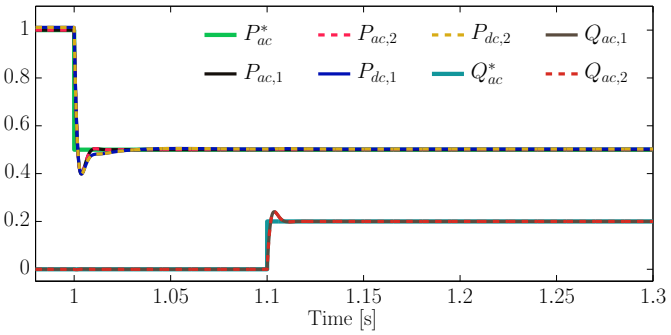


Figure 13: AC active and reactive power and DC power comparisons [pu] — 1: Modified Balanced W^{Δ}, 2: Balanced W^{Δ}

D. Simulation results

The two developed control structures are applied to the simulation of an MMC model. The same events as Section II are tested with the Modified Balanced W^{Δ} Control (Case1) and Balanced $\boldsymbol{i}_{diff_{ac}}$ (Case2). Fig. 13 shows the responses to the step change of the active and reactive power references. Unlike the case with the classic control (Fig. 8), no oscillation is observed on the DC power for both cases as expected. Fig. 14 shows the dynamics of the energy difference during the events. As it is observed, the energy difference is correctly regulated and converged to the reference value of zero after a short time. The Case2 takes slightly longer time due to the interactions from the other phases, which exert a modification from the expected active power exchange. In Fig. 15, the differential currents are depicted. For both cases, fundamental-frequency components are observed. Nonetheless, they have no impact on the DC power. This proves the effectiveness of the proposed control structures which enable to regulate the energy difference without having any interaction with DC side and allows to treat them internally.

IV. Conclusion

In this paper, control strategies of energy difference of the MMC have been analyzed. While maintaining the cascaded control structure, two structures of energy difference controllers have been presented. The proposed controllers allow regulating the energy difference by generating balanced differential current references. Simulation results have shown the effectiveness of the proposed controllers which enable to regulate the energy difference without having any interaction with the DC and AC grid. This implies that the regulation of the energy difference is treated as internal dynamics and can be dissociated from the global system in large-scale dynamics studies.

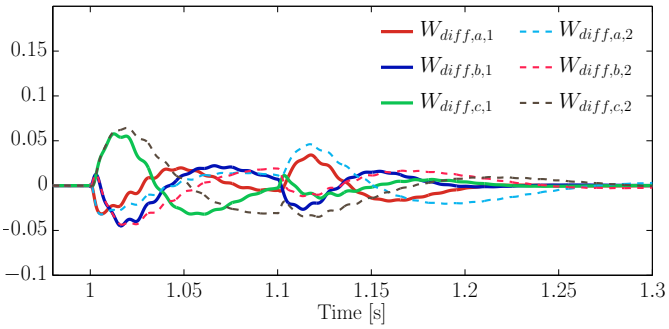


Figure 14: W^{Δ} comparison (filtered) [pu] — 1: Modified Balanced W^{Δ}, 2: Balanced W^{Δ}

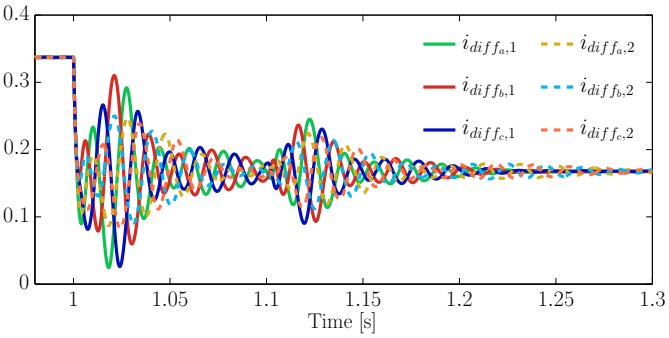


Figure 15: i_{diff} comparison [pu] — 1: Modified Balanced W^{Δ}, 2: Balanced W^{Δ}

References

[1] A. Lesnicar and R. Marquardt, "An innovative modular multilevel converter topology suitable for a wide power range," in *Power Tech Conference Proceedings, 2003 IEEE Bologna*, vol. 3, pp. 6 pp. Vol.3–, June 2003.

[2] A. Antonopoulos, L. Angquist, and H.-P. Nee, "On dynamics and voltage control of the modular multilevel converter," *2009 13th Eur. Conf. Power Electron. Appl.*, 2009.

[3] S. Debnath, J. Qin, B. Bahrani, M. Saeedifard, and P. Barbosa, "Operation, control, and applications of the modular multilevel converter: A review," *IEEE Transactions on Power Electronics*, vol. 30, pp. 37–53, Jan 2015.

[4] H. Saad, X. Guillaud, J. Mahseredjian, S. Dennetière, and S. Nguefeu, "Mmc capacitor voltage decoupling and balancing controls," in *Power Energy Society General Meeting, 2015 IEEE*, pp. 1–1, July 2015.

[5] P. Munch, D. Gorges, M. Izak, and S. Liu, "Integrated current control, energy control and energy balancing of modular multilevel converters," in *IECON 2010 - 36th Annual Conference on IEEE Industrial Electronics Society*, pp. 150–155, Nov 2010.

[6] S. Wenig, F. Rojas, K. SchÃűnleber, M. Suriyah, and T. Leibfried, "Simulation framework for dc grid control and acdc interaction studies based on modular multilevel converters," *IEEE Transactions on Power Delivery*, vol. 31, pp. 780–788, April 2016.

[7] G. Bergna, E. Berne, P. Egrot, P. Lefranc, A. Arzande, J.-C. Vannier, and M. Molinas, "An energy-based controller for hvdc modular multilevel converter in decoupled double synchronous reference frame for voltage oscillation reduction," *Industrial Electronics, IEEE Transactions on*, vol. 60, pp. 2360–2371, June 2013.

[8] P. Delarue, F. Gruson, and X. Guillaud, "Energetic macroscopic representation and inversion based control of a modular multilevel converter," in *Power Electronics and Applications (EPE), 2013 15th European Conference on*, pp. 1–10, Sept 2013.

The author has requested enhancement of the downloaded file. All in-text references underlined in blue are linked to publications on ResearchGate.